Journal of Rock Mechanics and Geotechnical Engineering 10 (2018) 935–946

Contents lists available at ScienceDirect

Journal of Rock Mechanics and Geotechnical Engineering

journal homepage: www.rockgeotech.org

Full Length Article

Bearing behavior and failure mechanism of squeezed branch piles

Minxia Zhang [a], Ping Xu [a,*], Wenjie Cui [a], Youbin Gao [b]

[a] School of Civil Engineering, Henan Polytechnic University, Jiaozuo, 454003, China
[b] School of Water Conservancy and Environmental Engineering, Zhengzhou University, Zhengzhou, 450002, China

ARTICLE INFO

Article history:
Received 1 August 2017
Received in revised form
9 November 2017
Accepted 19 December 2017
Available online 23 June 2018

Keywords:
Squeezed branch piles
Field test
Bearing behavior
Failure mechanism
Numerical simulation

ABSTRACT

The current practice for the design of squeezed branch piles is mainly based on the calculated bearing capacity of circular piles. Insufficient considerations of the load-transfer mechanism, branch effect and failure mechanism, as well as overreliance on pile load tests, have led to conservative designs and limited application. This study performs full-scale field load tests on instrumented squeezed branch piles and shows that the shaft force curves have obvious drop steps at the branch position, indicating that the branches can effectively share the pile top load. The effects of branch position, spacing, number and diameter on the pile bearing capacity are analyzed numerically. The numerical results indicate that the squeezed branch piles have two types of failure mechanisms, i.e. individual branch failure mechanism and cylindrical failure mechanism. Further research should focus on the development of the calculation method to determine the bearing capacities of squeezed branch piles considering these two failure mechanisms.

1. Introduction

Pile foundations play an important role in supporting structural loads when shallow foundations cannot provide sufficient bearing capacity or where the settlement is a major concern. More efficient foundation design will help to reduce construction costs and contribute to faster construction. Obviously, geotechnical engineers should develop new foundation concepts if foundation costs are to be reduced (Byrne and Houlsby, 2015). In consequence, many new pile foundation techniques have been proposed based on conventional concepts, by changing pile sectional shape to take advantage of foundation soil (rock) and pile bearing capacities, and adopting potential pile materials for more effective reinforcement at lower cost. For instance, engineers have already made full use of pile geometries to improve the axial load capacity of piles, such as tapered pile (Wei and El Naggar, 1999; El Naggar, 2004), pipe pile (Lehane and Gavin, 2001), helical pile (Elsherbiny and El Naggar, 2013; Byrne and Houlsby, 2015; Khazaei and Eslami, 2017), X-shaped pile (Lu et al., 2012; Zhou et al., 2017), Y-shaped pile (Lu et al., 2016), squeezed branch pile, and so on, which are all successful examples of pile geometry modification.

The squeezed branch pile was developed from the conventional circular pile (Yang et al., 1999). It contains a central rounded shaft with at least one branch (enlarged part) located on the shaft based on the distribution of soil strata, as shown in Figs. 1 and 2. Generally, the branch or plate is penetrated into the relatively hard soil layer using the hydraulic squeezed machine (Fig. 3). The three-dimensional (3D) static pressure is applied to the soil around each branch or plate. Thus, pile expansion cavity, soil compaction, pile cavity perfusion and branch integration in the pile all affect the pile-soil bearing behavior.

The squeezed branch piles are significantly more efficient than conventional circular piles. Hence, many theoretical analyses, and laboratory and in situ experiments have been conducted to investigate the pile bearing behavior and calculate the bearing capacities of squeezed branch piles. Qian (2003) and Qian et al. (2005) investigated the loading transfer behavior of squeezed branch piles under static load and exciting force of earthquake. In their studies, the influential factors of squeezed branch piles were analyzed. Yuan et al. (2006) compared the bearing capacities of squeezed branch pile, squeezed plate pile and conventional circular pile through field investigation. They suggested that the squeezed branch pile was the most efficient one among them, followed by the

* Corresponding author.
E-mail address: hpuxuping@126.com (P. Xu).
Peer review under responsibility of Institute of Rock and Soil Mechanics, Chinese Academy of Sciences.

https://doi.org/10.1016/j.jrmge.2017.12.010

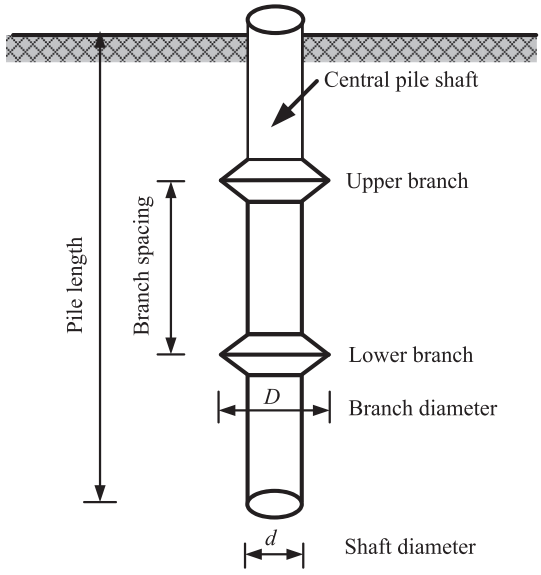

Fig. 1. Schematic diagram of squeezed branch pile.

squeezed plate pile and conventional circular pile. For example, a pile foundation project in the Eastern Expressway of Ningbo, China showed that the squeezed branch piles can save over 30% construction materials compared to conventional straight piles, while achieving the same compressive bearing capacity (Yuan et al., 2014). Furthermore, the squeezed branch piles were also found to be effective in anti-pulling as well as resisting axial compression (Qian, 2003; Gao, 2007; Gao et al., 2007; Zhang et al., 2008). Gao (2007) and Gao et al. (2007) investigated the squeezed branch pile responses in collapsible loess through field load test, and showed an excellent response under lateral loading, suggesting that the squeezed branch piles were reliable and excellent for collapsible loess. The squeezed branch piles provide improved vertical and horizontal bearing, as well as anti-pulling capacities, because the branches can provide greater frictional resistance.

Although the squeezed piles have been used for a considerable time, there is sparse information available on branch-soil-pile interaction and failure mechanisms, due to the fact that they are not widely used around the world. Therefore, further study is required on squeezed branch pile characteristics and bearing capacity.

This paper aims to evaluate the bearing responses of squeezed branch piles, and to explore the effects of branch position, spacing, number and diameter on pile bearing capacity. We also investigate the soil failure patterns around the branches. The results will provide valuable insight into underlying failure mechanism and load transfer regularity for squeezed branch piles.

2. Field test

2.1. Site description

This project is located at the top of the front alluvial fan of Taihang Mountain, China. The site has been surveyed by extensive investigation programs, including several field and laboratory tests. The area is mainly composed of clayey soil, with a silt and gravel layer of Quaternary alluvial deposit. The soil is divided into nine main layers from top to bottom (Nos. ①, ②, ③ and ⑤-⑩) and eight substrata (Nos. ⑤$_1$, ⑤$_2$, ⑥$_1$, ⑦$_1$, ⑧$_1$, ⑨$_1$, ⑨$_2$ and ⑩$_1$). Field and laboratory tests are performed for soil properties at different depths, as shown in Table 1.

The squeezed branch piles with 0.7 m in diameter and 32 m in effective length are investigated in this study, and each pile has two branches of 1.4 m in diameter. All piles are constructed using C40 grade concrete.

Fig. 2. Photo of excavated branch pile (Gao et al., 2009).

Fig. 3. Hydraulic squeezed machine.

Table 1
Geotechnical characteristics of the test site.

Soil layer	Water content, w (%)	Unit weight, γ (kN/m^3)	Void ratio, e	Liquid limit, W_L (%)	Plastic limit, W_P (%)	Liquidity index, I_L (%)	Plastic index, I_P (%)	Compression modulus, E_{s1-2} (MPa)	Bearing capacity, f_{ak} (kPa)
②	26.3	19.7	0.912	30.1	18.4	0.63	11.7	4.5	8
③	21.1	20.7	0.67	24.1	16.3	0.17	7.8	6	130
⑤	24.1	20.1	0.793	34.8	20	0.55	11.5	7.3	150
⑤$_1$	23.5	20	0.769	28.5	17.9	0.6	10.6	7.5	170
⑤$_2$	24.2	20.1	0.776	28.3	17.3	0.63	11	7	140
⑥	20.5	20.6	0.739	28.7	16.8	0.3	11.9	10	200
⑥$_1$	23.3	20.5	0.63	26.9	16.8	0.46	10.1	12	220
⑦	23	21.5						20	350
⑦$_1$	19.7	20.9	0.54					18	180
⑧	24.6	20.1	0.806	28.4	17.2	0.69	11.2	8.5	160
⑧$_1$		21.2						20	300
⑨	24.8	20	0.695	29.9	17.4	0.62	12.5	11	210
⑨$_1$		24.8						11	350
⑨$_2$		21.2						19.5	300
⑩	24.4	20.2	0.675	28.7	17.6	0.62	11.1	11	230
⑩$_1$		21.2						20	300

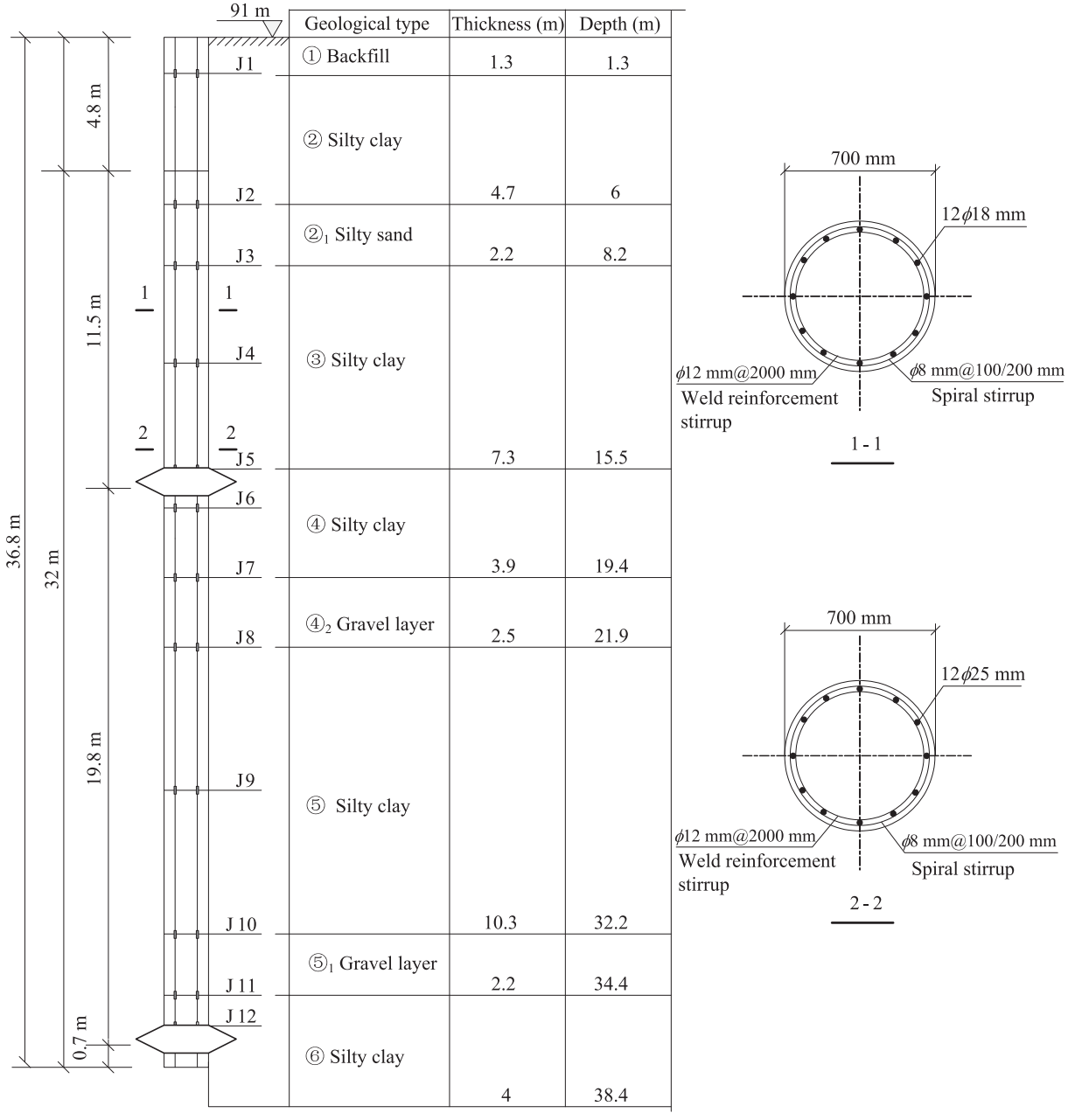

Fig. 4. Layout of vibrating strain gages and reinforcement drawing (J1-J12: positions of vibrating strain gages).

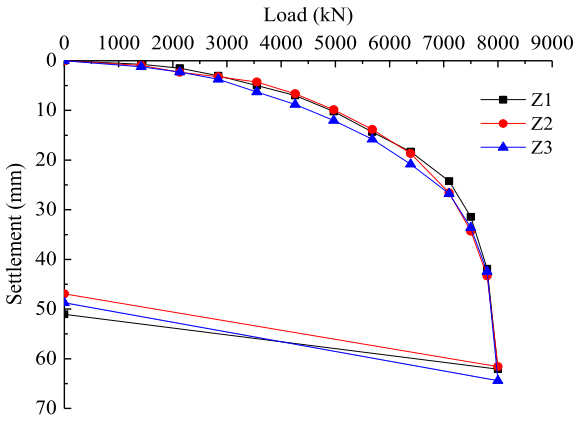

Fig. 5. Load-settlement curves of test piles.

2.2. Test pile instrumentation layouts

To examine the bearing behavior and axial stress distribution of test piles, 24 vibrating strain gages are cast into each test pile at locations corresponding to the adjacent soil layers. The strain gages are oriented parallel to the pile axis and centered on opposing pile faces, as shown in Fig. 4.

2.3. Static test results

2.3.1. Load-settlement behavior

Fig. 5 presents the load-settlement behaviors of three squeezed branch piles (Nos. Z1, Z2 and Z3 in Table 2) subjected to vertical load. The load-settlement curves vary gradually, without any apparent mutation points, indicating that the squeezed branch piles have reliable and stable bearing capacities. From test data (Table 2) and load settlement curves, the bearing capacities of test piles Z1, Z2 and Z3 are 7746 kN, 7689 kN and 7717 kN (pile in construction length, corresponding to 40 mm settlement (JGJ 106-2003, 2003)), and 7409 kN, 7379 kN and 7395 kN (pile in design length), respectively, minus the ultimate friction resistance from the natural ground to the pile top. The ultimate bearing capacity of a single pile is $Q_{uk} = 7394$ kN, which is the average ultimate bearing capacity of three squeezed branch piles.

2.3.2. Transfer regularity of pile shaft force

Fig. 6 shows the shaft force transfer curves for piles Z1, Z2 and Z3. The curves all exhibit two drop steps, i.e. step 1 corresponding to the position of the upper branch, and step 2 the lower branch. Step 1 comes from the first load (1000 kN), and step 2 from the third load (3000 kN). The curve slope of step 1 is less than that of step 2, which indicates that the bearing capacity of upper branch occurs earlier and is higher than that of lower branch. Thus, branch position is very important to the branch bearing behavior, which shows temporal and sequence effects.

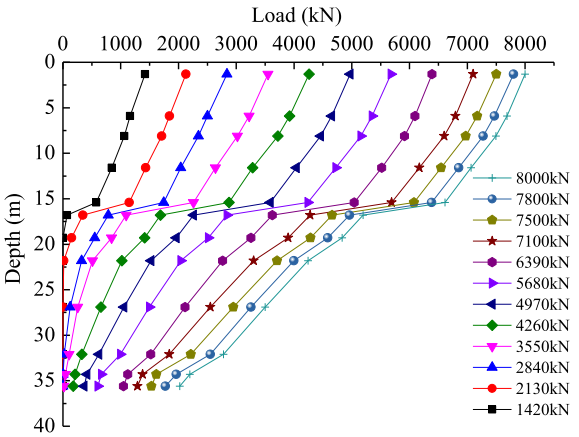

(a) Z1.

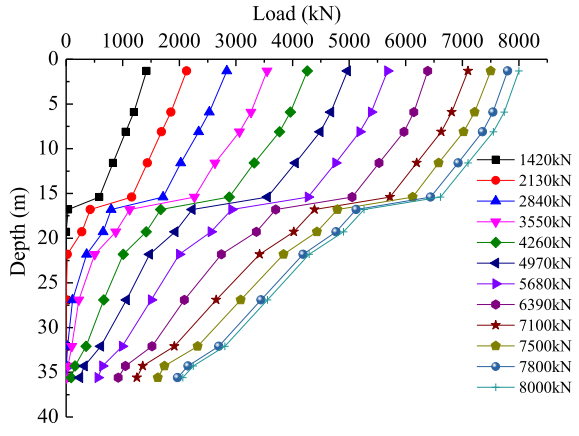

(b) Z2.

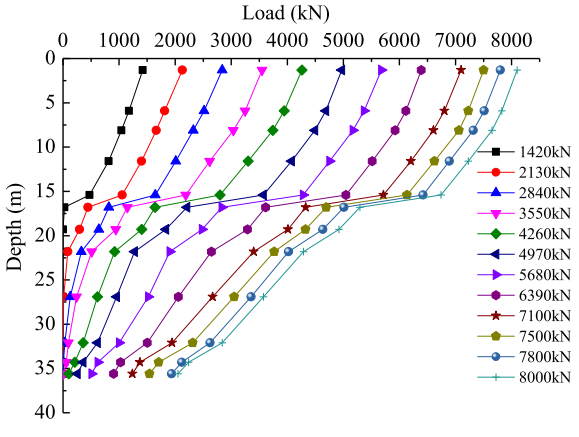

(c) Z3.

Fig. 6. Axial force distributions of piles.

Table 2
Static load test results.

Pile No.	Diameter (mm)	Length (m)	Maximum load (kN)	Maximum settlement (mm)	Ultimate bearing capacity in construction (kN)	Settlement (mm)	Design ultimate bearing capacity (kN)	Residual settlement (mm)
Z1	700	36.8	8000	62.1	7746	40	7409	51.06
Z2	700	36.8	8000	61.57	7689	40	7379	46.93
Z3	700	36.8	8100	64.42	7717	40	7395	48.73

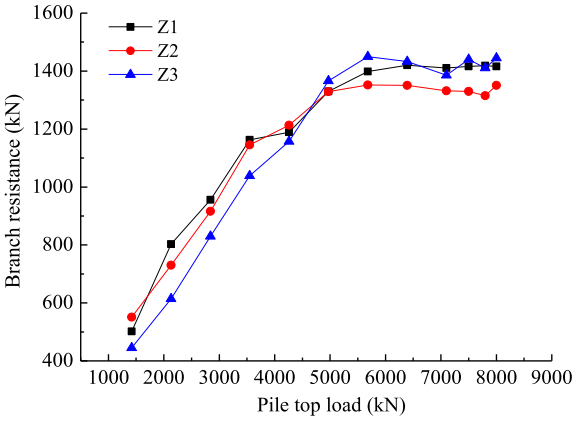

Fig. 7. Relationships between branch resistance and pile top load.

Table 3
Details of simulation cases.

Factor	Number of branch	Pile length (m)	Shaft diameter (m)	Number of cases	Remark
Branch position	1	32	0.7	6	Branch depth: 7 m, 12 m, 17 m, 22 m, 27 m and 32 m
	1	32	0.7	5	Distance from branch to pile tip: 0.5*D*, 1*D*, 2*D*, 3*D* and 4*D*
Branch spacing	2	32	0.7	7	Branch spacing: 1*D*, 2*D*, 3*D*, 4*D*, 5*D*, 6*D* and 7*D*
Branch number	1 2 3	32	0.7	3	
Branch diameter	2	32	0.7	3	Branch diameter: 2*d*, 2.5*d* and 3*d*

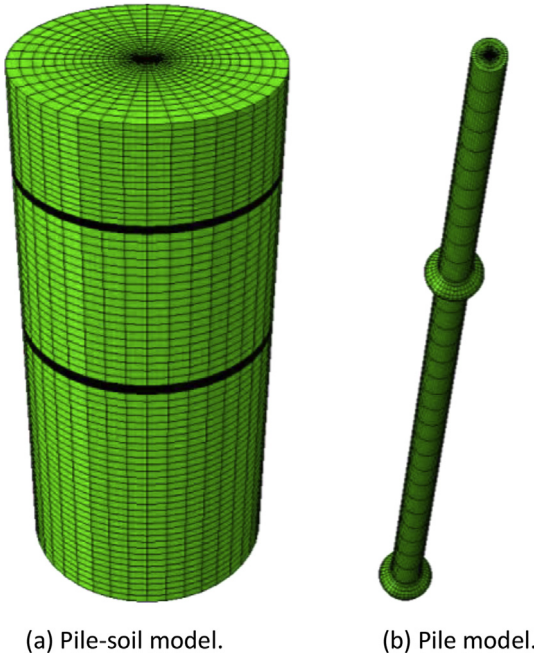

Fig. 8. Finite element model of squeezed branch pile.

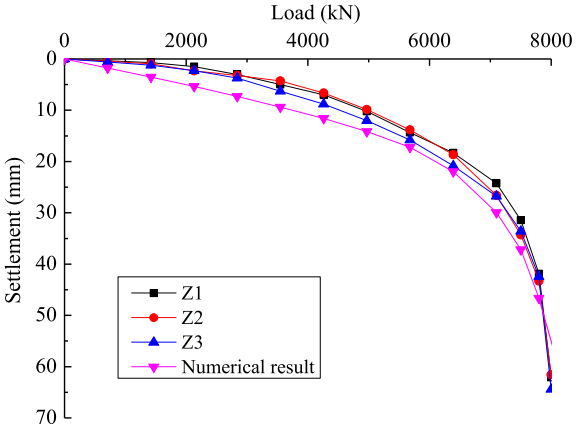

Fig. 9. Comparison of pile top load-settlement relationships obtained from field test with numerical result.

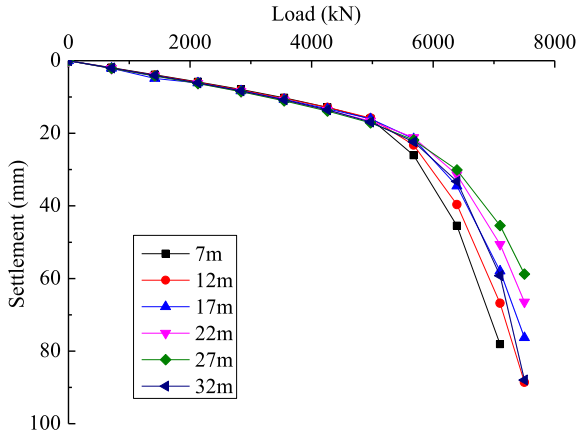

Fig. 10. Load-settlement curves of piles with different positions of branch.

Fig. 7 shows the relationship between the branch resistance and pile top load. The curves can be divided into three stages by pile top loads of 3550 kN and 6390 kN. The load shared by the branch increases quickly and linearly in the first stage, and then gradually develops in the second stage. The load sharing basically remains almost unchanged in the third stage.

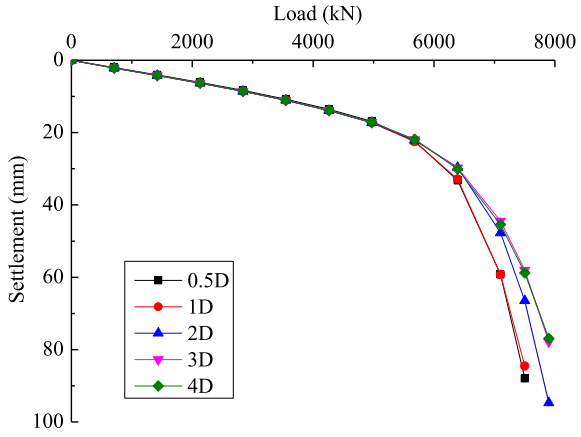

Fig. 11. Load-settlement curves of piles at different branch-to-pile tip distances.

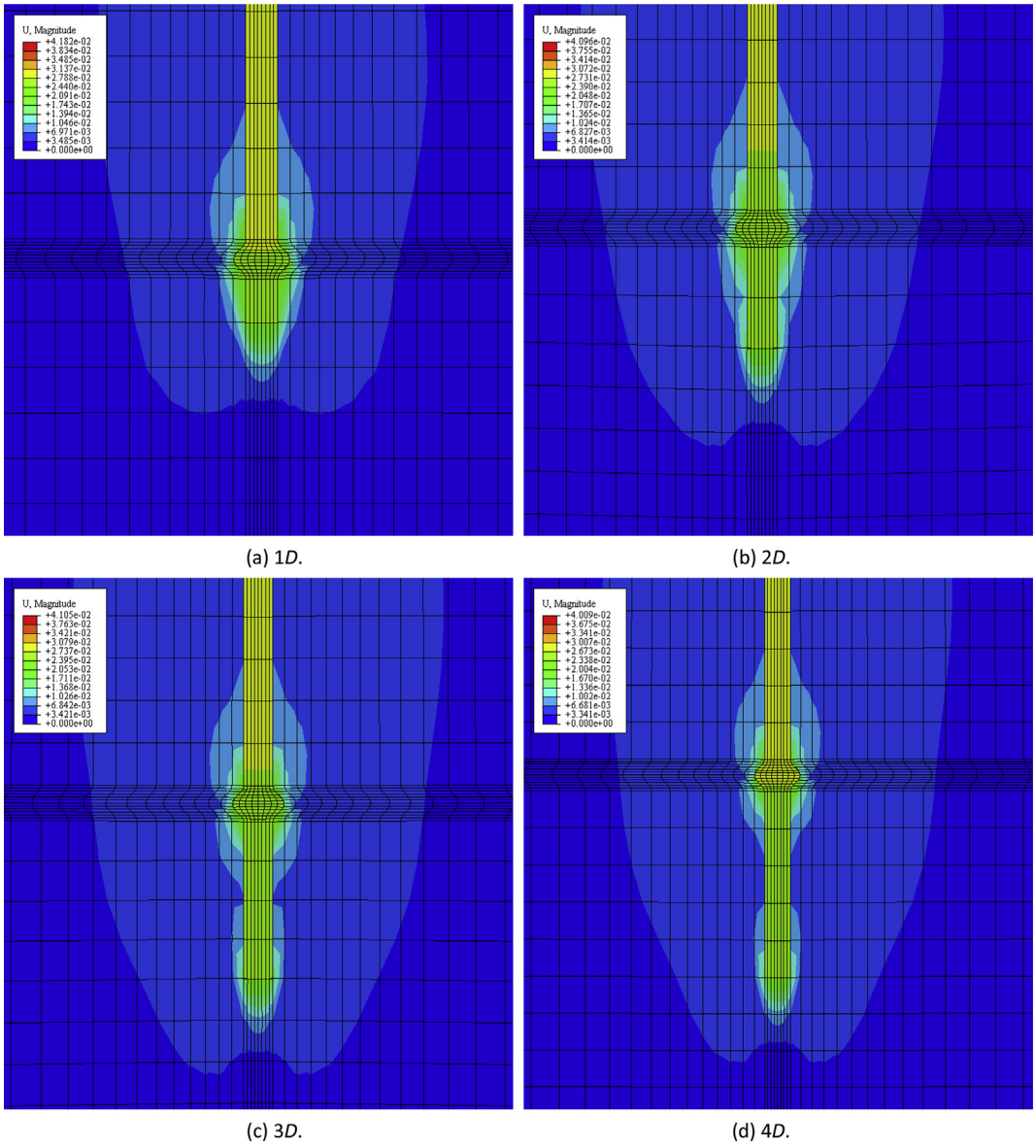

Fig. 12. Soil displacement contours around squeezed branch piles at different branch-to-pile tip distances (unit: m).

3. Branch effects on squeezed branch piles

3.1. Numerical modeling

The 3D simulation software Abaqus is employed to investigate the effects of branch position, spacing, number and diameter on the pile bearing capacity. Moreover, the branch effects on the ultimate bearing capacity and failure mechanism of pile are also interesting topics for investigation, while the failure mechanism is rarely reported in the literature. As a consequence, there is no accurate formula to be used to calculate the bearing capacity of squeezed branch piles, causing uneconomic design in most cases.

Model pile parameters are chosen to match the field test. The elastic modulus of the concrete pile is 30 GPa, the density is 2400 kg/m^3, and the Poisson's ratio is 0.2. For simplicity, the soil layers with similar properties are merged rationally. The dimensions of the model are 40 times the diameter of the pile by twice the length of the pile to avoid any significant boundary effect. The horizontal displacement constraint is applied to the cylindrical surface, and the vertical and horizontal displacement constraints are applied to the bottom of the model. The pile adopts linear elastic isotropic model. The elastic part of soil around pile is defined by elastic model, and the plastic part uses Mohr-Coulomb plastic model. The load is applied at the top of the pile cap using a "slowly maintaining load method" procedure.

Fig. 8 shows the finite element (FE) model of pile. To adapt to the dramatic changes of stress and strain and improve the accuracy of the calculation results, mesh geometry was parametrically defined to allow the possibility of geometrical variations when required, such as pile-soil contact surface and branch parameters.

As shown in Fig. 9, the load-settlement curves of squeezed branch piles obtained from the numerical simulation fit well with field test results, verifying that the numeric simulation is reliable.

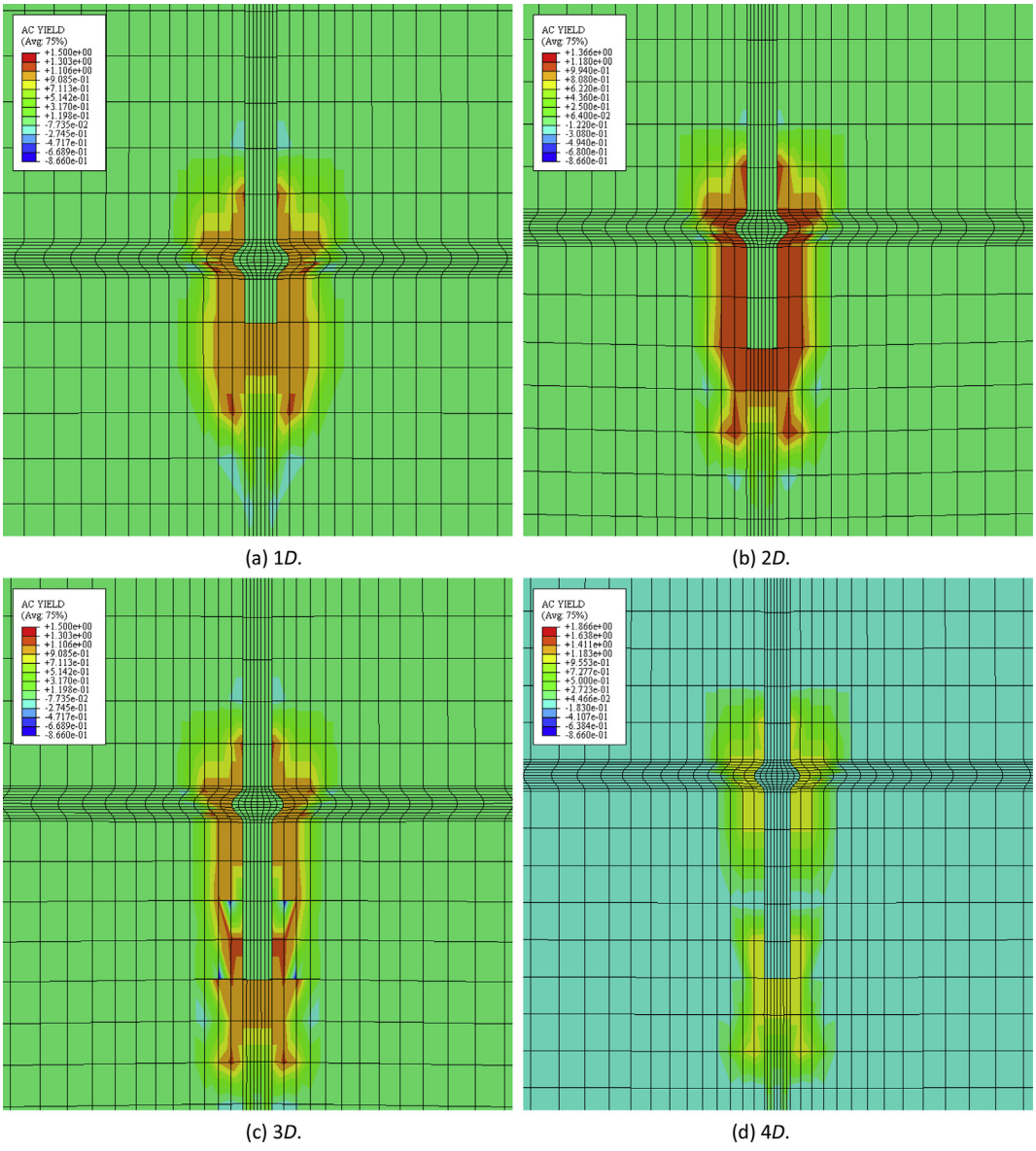

Fig. 13. Soil plastic deformation contours around squeezed branch piles at different branch-to-pile tip distances (unit: m).

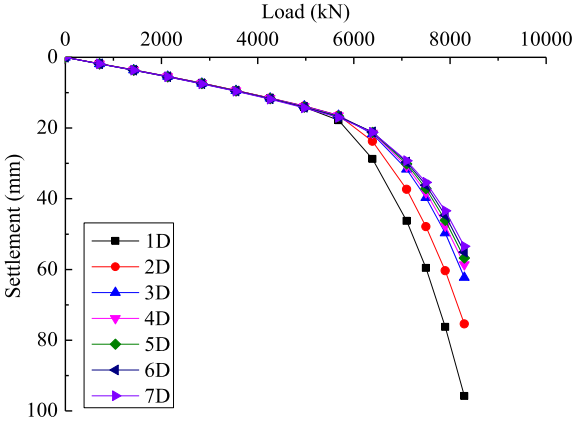

Fig. 14. Load-settlement curves of piles with different branch spacings.

3.2. Simulation cases

Four simulation cases are designed to study the influences of branch position, spacing, diameter and number. The soil is assumed to be homogeneous to study the effect of single variable and eliminate influences from other variables. The pile shaft diameter is $d = 0.7$ m and the branch diameter is $D = 2d = 1.4$ m by default if not specified. Table 3 summarizes the details of simulation cases.

3.3. Numerical results

3.3.1. Branch position

To investigate the branch effect on the performance of squeezed branch piles, six squeezed single-branch piles with different branch positions along the pile are analyzed. Fig. 10 shows the pile top load-settlement curves. The bearing capacities of six squeezed single-branch piles are 6212 kN, 6404 kN, 6603 kN, 6759 kN,

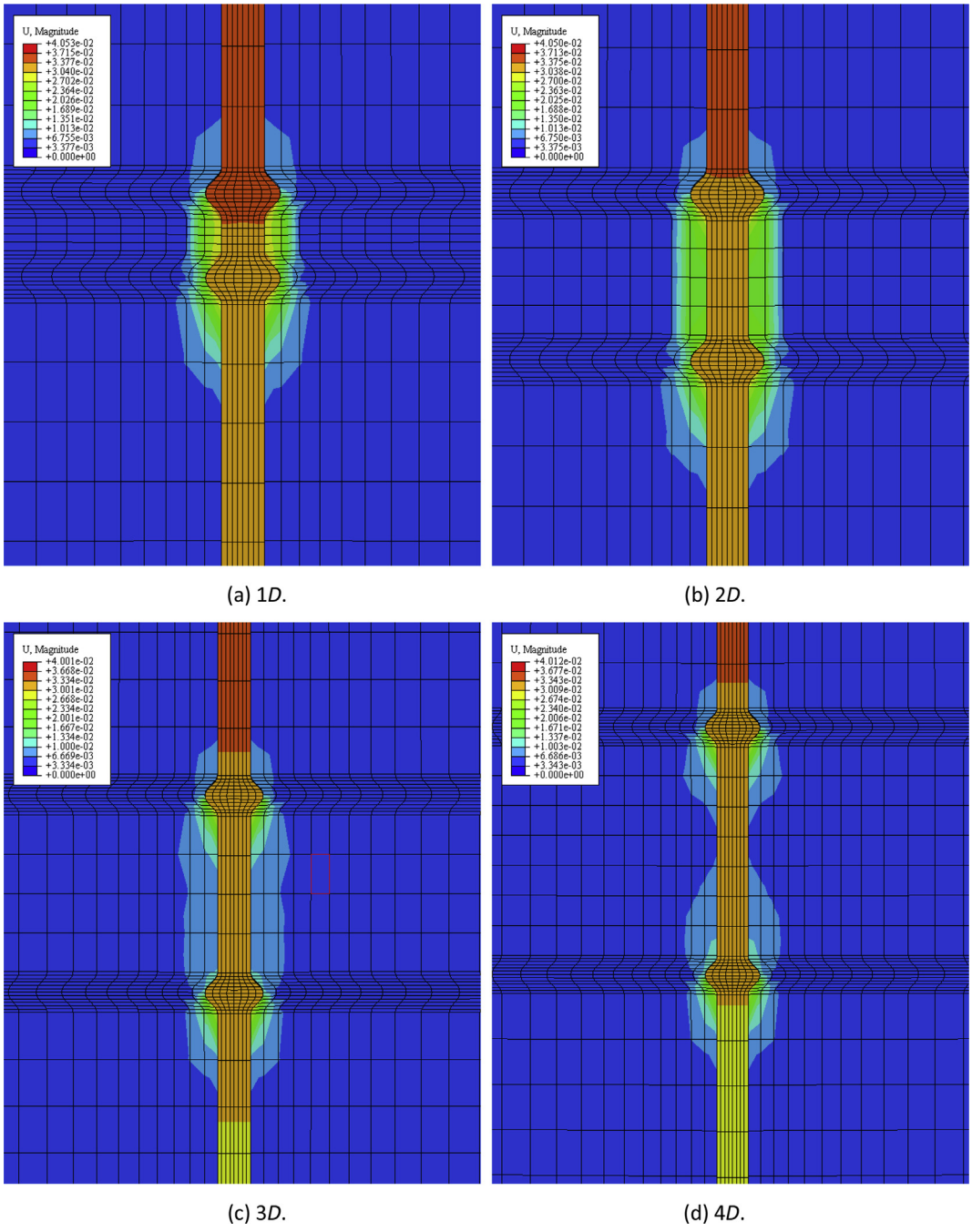

Fig. 15. Soil displacement contours around the piles with different branch spacings (unit: m).

6887 kN and 6617 kN, corresponding to branch positions of 7 m, 12 m, 17 m, 22 m, 27 m and 32 m, respectively. In the first five cases, the deeper the branch position is, the greater the pile bearing capacity is. However, in the last case, the ultimate bearing capacity is reduced and the pile settlement is increased, due to the fact that the branch is located at the pile tip.

Five values of distance from the branch to the pile tip (0.5*D*, 1*D*, 2*D*, 3*D* and 4*D*) are employed to examine the effect of branch position on the pile bearing capacity. The numerical results are shown in Fig. 11. We can see that the load-settlement curves of piles at the branch-to-pile tip distances of 3*D* and 4*D* are coincident with each other, but are significantly reduced at higher load and closer distances. Thus the optimal distance between branch and pile tip is at least 3*D*.

Fig. 12 shows the soil displacement contour around the pile under vertical ultimate load, with different branch-to-pile tip distances. When the branch-to-pile tip distances are equal to 1*D* and 2*D*, the soil displacement field caused by the branch is coincident with that around the pile tip, i.e. the branch and pile tip jointly share the load. However, when the branch-to-pile tip distance is

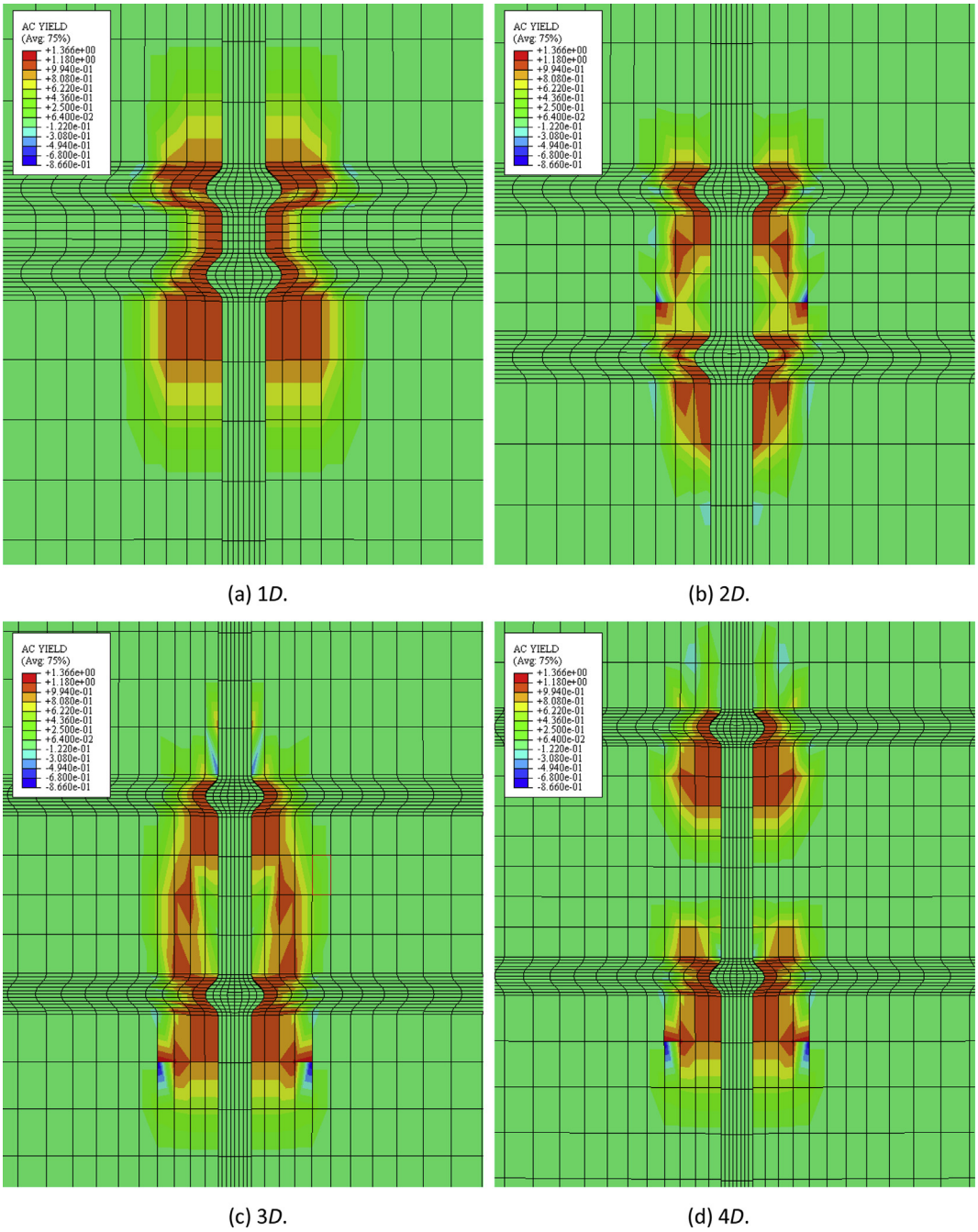

Fig. 16. Soil plastic deformation contours around the piles with different branch spacings (unit: m).

3*D*, it can be found that the soil displacement fields near the branch and pile tip are separated gradually. The branch and pile tip bear the load separately. Especially, when the branch-to-pile tip distance is 4*D*, the aforementioned soil displacement fields are separated more obviously.

Fig. 13 shows that the soil plastic deformation contours near the branch and pile tip exhibit similar variation as Fig. 12. When the branch-to-pile tip distances are 1*D* and 2*D*, the plastic deformation fields of soils around the branch and pile tip connect with each other, whereas at larger branch-to-pile tip distances (3*D* and 4*D*), soil plastic deformation fields around the branch and tip are separated, allowing independent load bearing.

3.3.2. *Branch spacing*

Fig. 14 shows the load-settlement curves of squeezed branch piles with different branch spacings. In these cases, the top branch is fixed, and at the same load level, one can see that with the increase in branch spacing, the ultimate bearing capacity of pile is gradually increased, but the increase rate becomes smaller and smaller. The results show that the ultimate bearing capacity of pile increases from 6887 kN to 7220 kN and 7536 kN (by 4.8% and 9.4%), respectively, when the branch spacing increases from 1*D* to 2*D* and 3*D*. As the branch spacing gradually increases from 3*D* to 7*D*, the ultimate bearing capacity of pile improves slightly.

Fig. 15 shows the soil displacement contours around the piles with different branch spacings. At smaller branch spacing, the soil

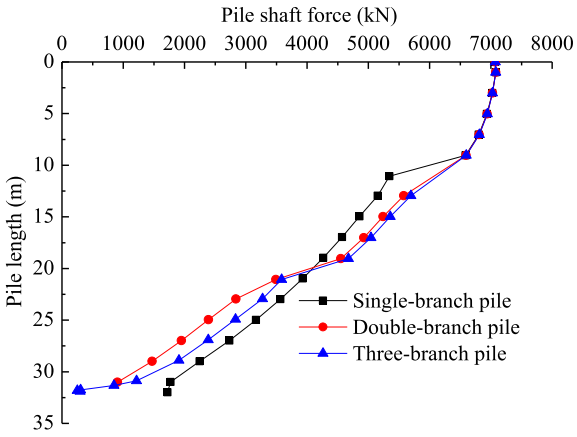

Fig. 17. Pile shaft force curves of squeezed branch piles.

displacement fields around the two branches connect with each other, whereas at larger branch spacing, separate displacement fields exist.

Fig. 16 shows the soil plastic deformation contours around the piles with different branch spacings. When the branch spacing is less than 3*D*, the soil plastic deformation fields around the branches connect with each other, indicating that the soils around the branches share the load jointly. At larger branch spacing, soil plastic deformation fields are separated, sharing the load separately. Thus the bearing capacity of the branch can be fully exerted when the branch spacing is 3*D* or larger, significantly improving overall pile bearing capacity. Larger branch spacing increases overall pile bearing capacity slightly, similar to the case in Section 3.3.1.

3.3.3. Branch number

In order to examine the effect of branch number on the pile bearing capacity, three types of squeezed branch piles are used, i.e. single branch, double branches and three branches. The ultimate bearing capacities of three piles are 6404 kN, 7740 kN and 8886 kN, respectively. Although they increase with increase in branch number, which is consistent with previous studies, the incremental difference decreases with increasing number of branches (1336 kN and 1128 kN, respectively).

Fig. 17 shows the pile shaft force curves for squeezed multi-branch piles. Although their ultimate bearing capacities can be improved by increasing the number of branches, this will also greatly increase the cost, human resource requirement and construction difficulty. When the branch number exceeds a certain value, the bearing capacity of single pile will be reduced.

3.3.4. Branch diameter

We calculate the load-settlement curves of piles with $D = 2d$, $2.5d$ and $3d$, as shown in Fig. 18, with corresponding ultimate bearing capacities of 7740 kN, 9188 kN and 10,572 kN, respectively. When $D = 3d$, pile settlement reaches 40 mm (Fig. 18), and the load-settlement curve changes slowly, indicating that the pile ultimate bearing capacity has not been reached. Since the safety of buildings is greatly influenced by settlement, the pile's larger potential bearing capacity could never be approached, and the cost of fabricating the larger-diameter pile would be wasted.

Fig. 19 shows the axial force curves for piles with different branch diameters. At the same load level, larger-diameter branches correspond to larger shares of the overall load, which will increase the load sharing ratio and reduce the axial force transmitted to the pile tip.

4. Failure mechanisms of squeezed branch piles

The failure mechanisms of squeezed branch pile have drawn considerable attention in analysis and design of pile foundations. Two failure mechanisms of squeezed branches, i.e. individual branch failure mechanism and cylindrical shear failure mechanism, are proposed in this section.

Numerical results indicate that an individual soil failure surface is developed below the branch during compression, for single- or multiple-branch piles with branch spacing larger than 3*D*. Comparing Figs. 12, 13, 15b and d, under compression, each branch has independent displacement and plastic deformation contours, i.e. squeezed branch piles have an individual branch failure mechanism, as shown in Fig. 20a.

Figs. 15a–c and 16a–c show that the squeezed branch piles with branch spacing no more than 3*D* generate cylindrical and plastic displacement contours under ultimate compression, i.e. the squeezed branch piles generate a cylindrical shear failure surface (Fig. 20b) when subjected to ultimate compressive load.

Development of individual (Fig. 20a) or cylindrical (Fig. 20b) shear failure mechanisms would depend greatly on soil type and spacing ratio, S/D, where S is the spacing between adjacent branches. Therefore, both failure mechanisms should be considered to evaluate the bearing capacities of squeezed branch piles.

For the individual branch failure mechanism, the ultimate bearing capacity of pile will principally depend on friction along the

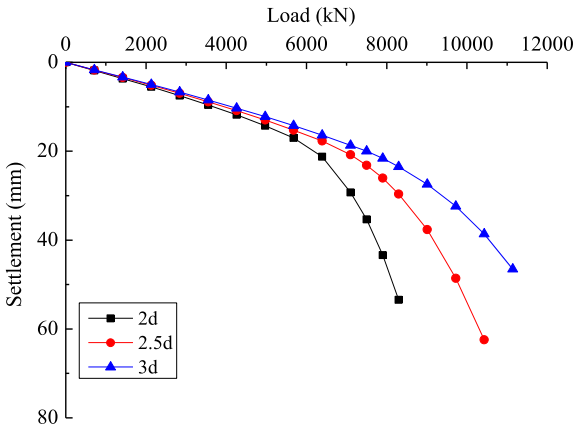

Fig. 18. Load-settlement curves of piles with different branch diameters.

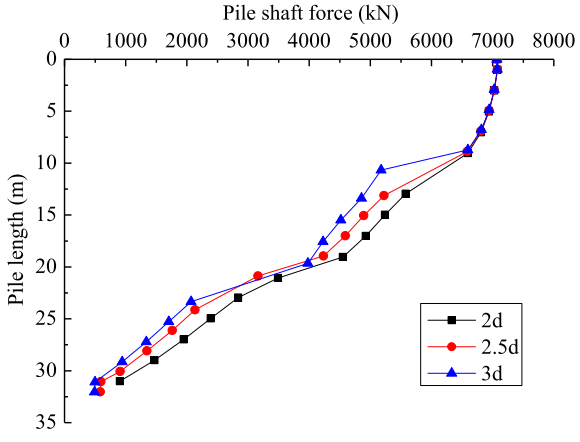

Fig. 19. Axial force distribution of piles with different branch diameters.

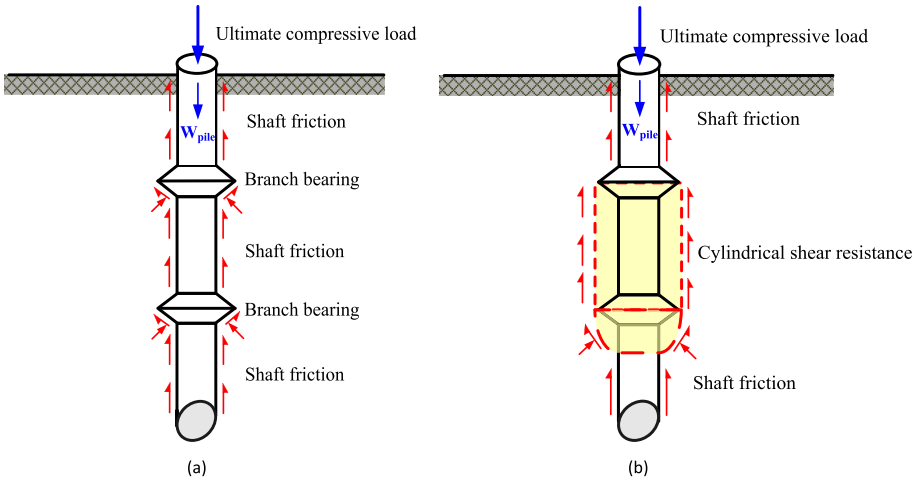

Fig. 20. Possible failure mechanisms for squeezed branch piles under compression: (a) Individual branch failure, and (b) Cylindrical shear failure.

shaft and bearing capacity of each branch, whereas for the cylindrical shear failure mechanism, soil-on-soil failure occurs at the (average) branch diameter. Depending on the depth of the lower branch, there may be a bearing failure at the lower branch or the cylindrical shear may extend to the pile tip. Contributions from shaft friction below the lower branch and pile end bearing should also be considered.

5. Conclusions

Field tests reveal important information with respect to squeezed branch pile performance. The effects of branch position, spacing, number and diameter on pile bearing capacity are analyzed numerically, and two failure mechanisms are proposed based on the soil displacement and plastic deformation fields. The following conclusions are derived:

(1) The load-settlement curves for the three field test piles do not have apparent mutation points and exhibit slow transformation. The ultimate bearing capacities of the test piles (Nos. Z1, Z2 and Z3) are 7409 kN, 7379 kN and 7395 kN, respectively, with an average ultimate bearing capacity of 7394 kN. Hence, the squeezed branch piles have excellent bearing capacity.

(2) Field test confirms that the squeezed branch pile is a viable deep foundation option for support of heavily loaded structures. The experimental shaft force transfer curves are very similar and show significant drop steps at branch locations, with monotonically decreasing shaft forces to the pile tip. Thus, the branch shares a significant proportion of the transferred load, which greatly improves the bearing capacity of squeezed branch pile compared with conventional cylindrical pile.

(3) The effects of branch position, spacing, number and diameter on the pile bearing capacity are investigated numerically. The optimal branch design is determined as not more than three branches within 3D spacing, to address both economic and practical problems.

(4) Two failure mechanisms are proposed based on soil displacement and plastic deformation contours, including generation of a cylindrical soil failure contour between two adjacent branches, or individual failure contour around each branch under compression, depending on soil type and branch spacing ratio (S/D).

Further study is necessary to develop the calculation method for determining the pile bearing capacity considering the two proposed failure mechanisms, soil plastic deformation, soil type and branch spacing ratio.

Conflicts of interest

We wish to confirm that there are no known conflicts of interest associated with this publication and there has been no significant financial support for this work that could have influenced its outcome.

Acknowledgements

The work presented in this paper was supported by the National Natural Science Foundation of China (Grant Nos. U1404527 and 51508166) and Opening Laboratory for Deep Mine Construction of Henan Polytechnic University (2014KF-07). The first author was hosted as a visiting scholar at the University of Western Australia (UWA) during part of this work and would like to thank Prof. Barry Lehane of UWA for his kind guidance.

References

Byrne BW, Houlsby GT. Helical piles: an innovative foundation design option for offshore wind turbines. Philosophical Transactions of the Royal Society A Mathematical Physical and Engineering Sciences 2015;373(2035). https://doi.org/10.1098/rsta.2014.0081.

El Naggar MH. The 2002 Canadian Geotechnical Colloquium: the role of soil-pile interaction in foundation engineering. Canadian Geotechnical Journal 2004;41(3):485–509.

Elsherbiny ZH, El Naggar MH. Axial compressive capacity of helical piles from field tests and numerical study. Canadian Geotechnical Journal 2013;50(12):1191–203.

Gao X. Study on load bearing characteristic of squeezed branch and plate pile with full-scale test and numerical methods. PhD Thesis. Hangzhou: Zhejiang University; 2007 (in Chinese).

Gao X, Wang J, Zhu X. Static load test and load transfer mechanism study of squeezed branch and plate pile in collapsible loess foundation. Journal of Zhejiang University Science A 2007;8(7):1110–7.

Gao X, Li J, Wang W, Zhu X. Disscussion on formula of vertical bearing capacity of rotated branches pile in Luoyang. Rock and Soil Mechanics 2009;30(6):1676–80 (in Chinese).

JGJ 106-2003. Technical code for testing of building foundation piles. Beijing: China Building Industry Press; 2003 (in Chinese).

Khazaei J, Eslami A. Postgrouted helical piles behavior through physical modeling by FCV. Marine Georesources and Geotechnology 2017;35(4):528–37.

Lehane BM, Gavin KG. Base resistance of jacked pipe in sand. Journal of Geotechnical and Geoenvironmental Engineering 2001;127(6):473–80.

Lu Y, Liu H, Ding X, Kong G. Field tests on bearing characteristics of X-section pile composite foundation. Journal of Performance of Constructed Facilities 2012;26(2). https://doi.org/10.1061/(ASCE)CF.1943-5509.0000247.

Lu Y, Ng CWW, Lam SY, Liu H, Ding X. Comparative study of Y-shaped and circular floating piles in consolidating clay. Canadian Geotechnical Journal 2016;53(9):1483–94.
Qian D. Engineering application study of squeezed branch pile with high antipulling behavior. Chinese Journal of Rock Mechanics and Engineering 2003;22(4):678–82 (in Chinese).
Qian D. Study on bearing behavior of squeezed branch pile. Chinese Journal of Rock Mechanics and Engineering 2003b;22(3):494–9 (in Chinese).
Qian D, Zhao Y, Wang D. Experimental study on the dynamic interaction of squeezed branch pile-soil-structure system by shaking table test. Journal of Shanghai Jiaotong University 2005;39(11):1856–61 (in Chinese).
Wei J, El Naggar MH. Experimental study of axial behaviour of tapered piles: reply 1. Canadian Geotechnical Journal 1999;36:1204–5.
Yang J, Cui J, Tang Y. Site test research of reinforced concrete root piles cast in place. Industrial Construction 1999;29(10):49–51 (in Chinese).
Yuan H, Hang Y, Qu Z. Experimental study of the carrying capacity of the change section pile. Journal of Beijing University of Technology 2006;32(10):879–82 (in Chinese).
Yuan L, Dai G, Gong W. Experimental investigation, calculation and analysis of compressive bearing capacity of squeezed branch piles. Hans Journal of Civil Engineering 2014;3:103–9.
Zhang Y, Yuan H, Qu Z, Gao H. Experimental study on the anti-pulling behavior of the squeezed cast-in-place pile. Engineering Mechanics 2008;25(Supp. 1):82–5 (in Chinese).
Zhou H, Liu H, Randolph MF, Kong G, Cao Z. Experimental and analytical study of X-section cast-in-place concrete pile installation effect. International Journal of Physical Modelling in Geotechnics 2017;17(2):103–21.

Minxia Zhang obtained her BSc and MSc degrees in Geotechnical Engineering from Fuzhou University, China, in 2002 and 2005, respectively, and her PhD in Geotechnical Engineering from Hohai University in 2011. At present, she is an associate professor at the Department of Civil Engineering, Henan Polytechnic University, China. Her current research interests include (1) experimental investigations on underground structure-soil interaction caused by mining, and (2) stability analysis of building foundation in mining area.